DAMAGE MECHANISM ANALYSIS OF 2D 1×1 BRAIDED COMPOSITES UNDER UNIDIRECTIONAL TENSION

Zhang Chao(张超), *Xu Xiwu*(许希武), *Chen Kang*(陈康)

(State Key Laboratory of Mechanics and Control of Mechanical Structures, Nanjing University of Aeronautics and Astronautics, Nanjing, 210016, P. R. China)

Abstract: Coupling with the periodical displacement boundary condition, a representative volume element (RVE) model is established to simulate the progressive damage behavior of 2D 1×1 braided composites under unidirectional tension by using the nonlinear finite element method. Tsai-Wu failure criterion with various damage modes and Mises criterion are considered for predicting damage initiation and progression of yarns and matrix. The anisotropic damage model for yarns and the isotropic damage model for matrix are used to simulate the microscopic damage propagation of 2D 1×1 braided composites. Murakami's damage tensor is adopted to characterize each damage mode. In the simulation process, the damage mechanisms are revealed and the tensile strength of 2D 1×1 braided composites is predicted from the calculated average stress-average strain curve. Numerical results show good agreement with experimental data, thus the proposed simulation method is verified for damage mechanism analysis of 2D braided composites.

Key words: 2D braided composites; representative volume element (RVE); failure modes; damage mechanism; strength prediction

CLC number: TB332 **Document code**: A **Article ID**: 1005-1120(2013)04-0317-11

INTRODUCTION

Weight reduction has a very special and important meaning for modern aircraft structure. Currently, the extent of fiber-reinforced composites applied in aircraft structures has become one of the most important targets making the advancement of modern structural design. As a kind of new and lightweight textile material, braided composites have tremendous potential applications in the aeronautics and astronautics industries. Besides all the advantages of the conventional laminated composites, braided composites have even better structural integrity, higher fatigue and impact resistance and lower production costs. Because of these broad potential benefits, braided composites are subjected to special concern now. Before braided composites are used in primary loading-bearing structures, a rational characterization of their mechanical properties is essential.

The spatial configuration of the braiding yarns is complex, but the microstructure of the composites shows a good periodicity. Thus, the mechanical properties of composites structures are often investigated through a representative volume element (RVE). Thus far, theoretical analysis and finite element method have been widely applied. Theoretical analysis is based on either iso-strain or iso-stress assumption. Aggarwal et al[1-2] proposed an analytical model to predict the in-plane stiffness and tension strength of 2D braided composites. In their model, the yarn undulations and inter yarn gaps were considered. Byun[3] introduced an analytical model to determine the three dimensional elastic properties of 2D flat braided composites using a volume avera-

Website of on-line first: http://www.cnki.net/kcms/detail/32.1389.V.20121226.0936.004.html (2012-12-26 09:36).

Foundation item: Supported by the National Natural Science Foundation of China (10672075).

Received date: 2012-01-12; **revision received date**: 2013-03-27

Corresponding author: Xu Xiwu, Professor, E-mail: xwxu@nuaa.edu.cn.

ging technique. Masters et al[4] investigated the mechanical properties of 2D triaxial braided composites experimentally; and then they used four different models: Laminate model, laminate correction model, diagonal brick model and finite element model to predict elastic constants respectively. Overall the finite element model provided the closest agreement to experimental results. Quek et al[5] first introduced the effect of initial micro-structural imperfections to the analytical model for the calculation of elastic stiffness of 2D triaxial braided composite. Some other researchers also have done much work on the effective elastic properties prediction of braided composites[6-9].

Although theoretical analysis is simple to implement, it can only yield the elastic constants but is difficult to exhibit the accurate micro stress distribution and the damage characteristics of the braided composites. On the other hand, the finite element method can overcome these limitations existing in the theoretical analysis and provide more information on the damage and failure characteristics. Therefore, besides the investigation on the stiffness properties[10-12], the strength and damage properties of braided composites have been received more attention by using the finite element method[13-21].

Potluri and Manan[13] presented a RVE model with lenticular tows cross-section to compute the stiffness and strength of 2D 1×1 braided composites based on linear analysis, however, the study on damage propagation in the composites was not reported. Tang et al[14] employed a bottom-up multi-scale finite element modeling method to simulate the progressive failure behavior of 2×2 braided composites. Quek et al[15-16] explored the compressive response and failure of 2D triaxial braided composites experimentally and found that the dominant failure mechanism of the composites was the buckling of yarns. A RVE model was established to predict the effective stiffness and strength of the braided composites subjected to compression load. Song et al[17-18] took an eigenvalue analysis of RVE of the 2D triaxial braided composites, and then selected the first eigenmode as the initial imperfections to simulate the compressive behavior of the composites. Li et al[19] proposed a RVE that involved the interface damage of yarns to predict the progressive damage evolution of 2D triaxial braided composites under unidirectional tension. The numerical results for stiffness and strength agreed well with the experimental data. In addition, the damage evolution simulations of 3D braided composites were performed in Refs. [20-22].

It is seen that much research has been done on the damage simulations of 2D triaxial, 2D 2×2 and 3D braided composites, but little attention has been paid to strength prediction and damage mechanism analysis of 2D 1×1 braided composites. In this study, a RVE-based finite element model, which truly reflects the microstructure of braided composites, is established. Coupling with the periodical boundary condition, the RVE is presented to simulate the damage propagation of 2D 1×1 braided composites under unidirectional tension. Tsai-Wu and Mises failure criteria are considered for predicting damage initiation and progression of yarns and matrix, respectively. The whole process of damage initiation, propagation and catastrophic failure is carried out and the damage mechanisms in the process are revealed in detail.

1 MICROSTRUCTURE ANALYSIS AND RVE MODEL

For 2D braid comprises, three common braided architectures are 1×1 braid, 2×2 braid, and 3×3 braid. In 1×1 braid each yarn crosses over and below one other yarn, in 2×2 braid each yarn crosses over and below two yarns, and in 3×3 braid each yarn passes over and then above three other yarns. In addition to the braiding yarns, axial yarns are often inserted for dimension stability and improve the mechanical properties in the longitudinal direction; this type of braid is called triaxial braid[23]. The braided architecture of a 2D 1×1 braided composite is depicted in Fig. 1. For

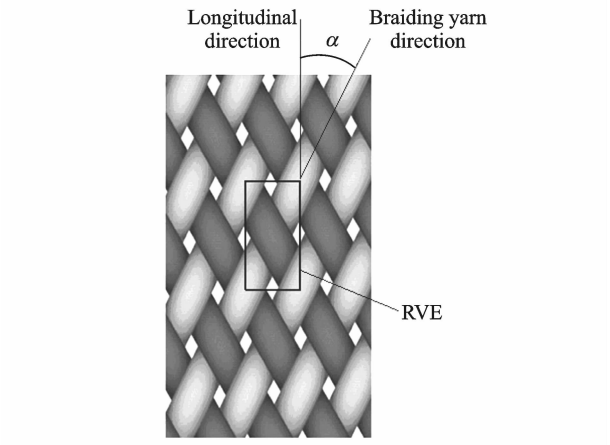

Fig. 1 2D 1×1 braided architecture

clarity, the matrix pockets are removed in Fig. 1. The angle between braiding yarns and the longitudinal direction, α, is called braid angle.

1.1 Basic assumptions

As a result of the repeating motion of yarn carriers, 1×1 braided composites have the smallest repeating structure. A RVE, shown in Fig. 1, is used to represent the 1×1 braided composites in the present study. The following assumptions are made in order to establish the micro-RVE model: (1) The cross-section shape of braiding yarns is flat hexagonal, as shown in Fig. 2; (2) the braiding yarns have the same structural parameters of width W, thickness t_b, and cross-sectional area A; (3) the yarns are uniform along the yarns′ direction; and (4) the small gaps between the adjacent yarns are negligible.

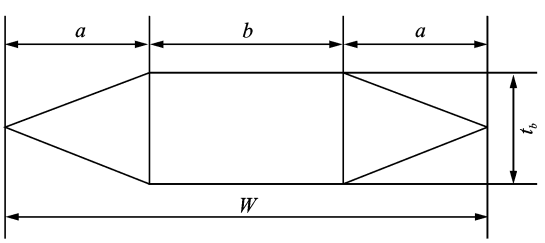

Fig. 2 Cross section sharp of braiding yarn

1.2 Structural parameters of RVE

From the cross section sharp of braiding yarn shown in Fig. 2, we have

$$W = 2a + b \tag{1}$$

$$A = (a + b)t_b \tag{2}$$

Fig. 3 shows the structural parameters on the cross section of 1×1 braided composites in the

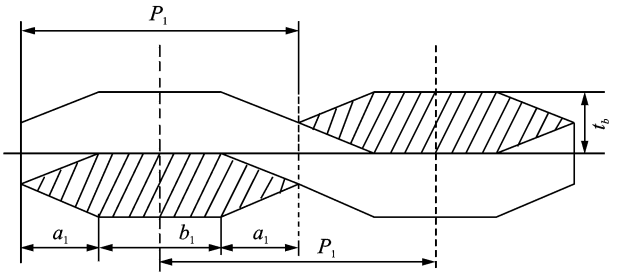

Fig. 3 Schematic section in yarn direction of 1×1 braided composites structure

braiding yarn direction. Note that some symbols used in Fig. 3 are slightly different from Fig. 2, namely, the width W of braiding yarn displayed in Fig. 2 is changed to P_1 in Fig. 3, and geometric parameters a and b in Fig. 2 are changed to a_1 and b_1. Their relations are as follows

$$P_1 = W/\sin 2\alpha \tag{3}$$

$$a_1 = a/\sin 2\alpha \tag{4}$$

$$b_1 = b/\sin 2\alpha \tag{5}$$

Make W_x, W_y and T represent the width, length and thickness of RVE, respectively, and they can be calculated by

$$W_x = W/\cos\alpha \tag{6}$$

$$W_y = W/\sin\alpha \tag{7}$$

$$T = 2t_b + t_m \tag{8}$$

where t_m is the thickness of pure matrix layers.

Fig. 4 gives the comparison of schematic diagram of actual intersecting braiding yarns and surface configuration of RVE. It is seen that the spatial configuration and the mutual squeezing of the yarns are validly reflected in the RVE model.

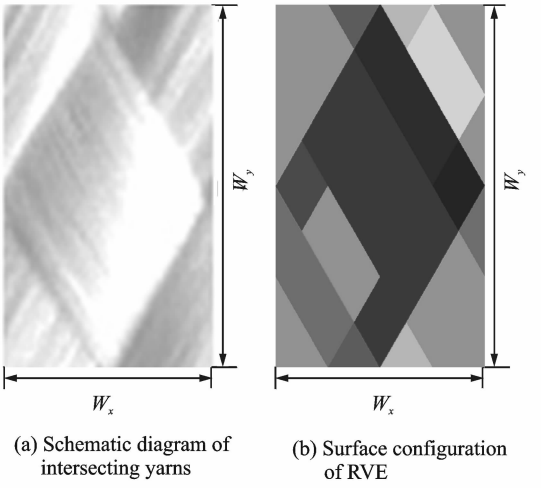

Fig. 4 Comparison of schematic diagram of intersecting yarns and surface configuration of structural RVE

2 FINITE ELEMENT MODEL

2.1 Periodic boundary condition and finite element meshing

2D braided composites are periodic structures consisting of periodic array of RVEs, so the periodical boundary conditions should be applied to the present damage simulation model which is based on the RVE model. That is to say, the progressive damage process of 2D braided composites is periodical. Displacement continuity conditions and traction continuity conditions must be satisfied at the opposite boundaries of the neighboring RVEs. Consequently, the unified periodical displacement boundary conditions proposed by Xia et al[24], which guarantee the two continuities conditions, are adopted.

In finite element software, periodic boundary condition is carried out by setting the linear constraint equations between master surface nodes and slave surface nodes. As shown in Fig. 5, three coordinate planes ($x_i = L_i$) are defined as master planes, and the nodes on them are called master nodes. Similarly, coordinate planes ($x_i = 0$) are slave planes and nodes on them are called slave nodes. The vertexes A, C, H are defined as reference points on which the displacement boundary condition is applied. The linear constraint equations between master nodes and slave nodes are expressed as

$$\begin{cases} u_i^{a'} = u_i^a + u_i^A \\ u_i^{c'} = u_i^c + u_i^C \\ u_i^{h'} = u_i^h + u_i^H \end{cases} \qquad i = x, y, z \tag{9}$$

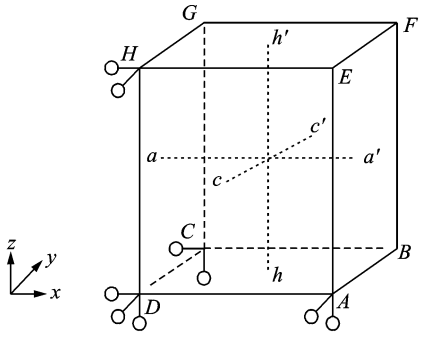

Fig. 5 Periodic boundary conditions

In order to satisfy the periodicity, the node distributions in the opposite paired faces of RVE should be identical. The meshed map method is used in the surface mesh and the periodic boundary conditions are imposed on the paired nodes by FORTRAN pre-compiler code.

Due to the complexity of the microstructure, 3D solid tetrahedral elements are adopted for the meshing of braiding yarns and matrix. The interfaces between the yarns and matrix are assumed to be perfectly bonded, that is to say, the damage mechanism of the interface debonding is ignored. Finite element meshes of the braiding yarns and the whole RVE model are shown in Fig. 6.

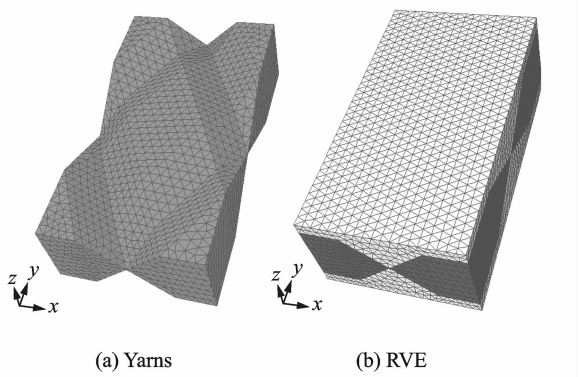

Fig. 6 Finite element meshes

2.2 Material properties of constituents

2D braided composites are composed of the braiding yarns and the resin matrix pockets. The material response of the constituents influences the macro-mechanical behavior of the composites. In this work, the resin matrix is assumed to be isotropic; the braiding yarns containing thousands of fibers and matrix are modeled as spatially undulating and transversely isotropic composites in local material coordinate system. The stiffness and strength properties of the braiding yarns can be calculated using the rule of mixture given by Chamis[25]. For the material orientation definition of every element in the braiding yarn, local L axis must follow the path curve, as shown in Fig. 7 (a), and the coordinate system of a yarn is given in Fig. 7 (b).

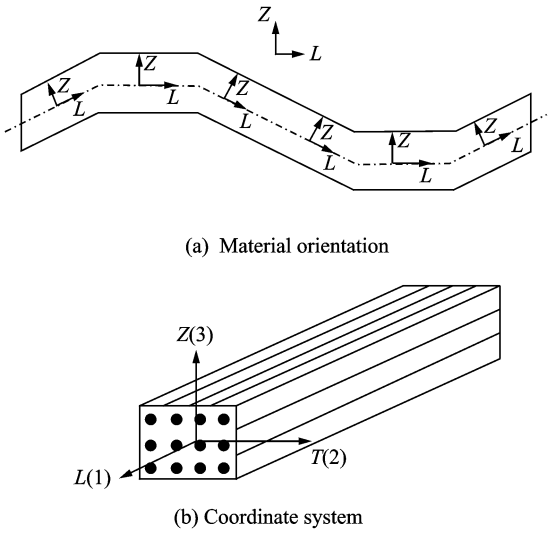

Fig. 7 Material orientation definition and coordinate system of braiding yarn

2.3 Constitutive relation of damaged material

The damage of yarns and matrix can be characterized by Murakami damage model. The damage model uses three principal damage variables to express the damage stations, which is expressed as[26]

$$\boldsymbol{D}=\sum_i D_i \boldsymbol{n}_i \otimes \boldsymbol{n}_i \qquad i=L,T,Z \tag{10}$$

where D_i and $\boldsymbol{n}_i$ are the principal value and principal unit vector of damage tensor, respectively.

The damage variables D_i mean the effective area reduction caused by micro-cracks and voids, and are given by

$$D_i=\frac{A_i-A_i^*}{A_i} \qquad i=L,T,Z \tag{11}$$

where A_i and A_i^* are total load bearing area and undamaged area, respectively.

The damage variables range from 0 to 1.0 according to damaged station. $D_i=0$ represents the initial undamaged materials and $D_i=1$ implies the completely damaged materials.

The effective stress is defined as

$$\sigma^*=\frac{1}{2}[(\boldsymbol{I}-\boldsymbol{D})^{-1}\sigma+\sigma(\boldsymbol{I}-\boldsymbol{D})^{-1}]=\boldsymbol{M}(\boldsymbol{D})\sigma \tag{12}$$

where σ^* is symmetric and $\boldsymbol{M}(\boldsymbol{D})$ the transformation matrix.

The constitutive equation of the damaged material is given by

$$\varepsilon=\boldsymbol{H}(\boldsymbol{D})\sigma \tag{13}$$

$\boldsymbol{H}(\boldsymbol{D})$ can be derived by the notion of energy identification, namely

$$\boldsymbol{H}(\boldsymbol{D})=(\boldsymbol{M}(\boldsymbol{D}))^{\mathrm{T}}:\boldsymbol{C}_0:\boldsymbol{M}(\boldsymbol{D}) \tag{14}$$

where $\boldsymbol{C}_0$ is the undamaged elastic tensor.

This, in turn, leads to the damaged stiffness matrix, which is the function of the undamaged elastic constants and the principal values of damage tensor, and is given by Ref. [27] as

$$\boldsymbol{C}(\boldsymbol{D})=\boldsymbol{H}^{-1}(\boldsymbol{D})=$$

$$\begin{Bmatrix} d_L^2C_{11} & & & & & \\ d_Ld_TC_{12} & d_T^2C_{22} & & & \text{sym} & \\ d_Ld_ZC_{13} & d_Td_ZC_{23} & d_Z^2C_{33} & & & \\ 0 & 0 & 0 & d_{TZ}C_{44} & & \\ 0 & 0 & 0 & 0 & d_{ZL}C_{55} & \\ 0 & 0 & 0 & 0 & 0 & d_{LT}C_{66} \end{Bmatrix} \tag{15}$$

where $d_L=1-D_L$, $d_T=1-D_T$, $d_Z=1-D_Z$, $d_{TZ}=\left(\frac{2d_Td_Z}{d_T+d_Z}\right)^2$, $d_{ZL}=\left(\frac{2d_Zd_L}{d_Z+d_L}\right)^2$, $d_{LT}=\left(\frac{2d_Ld_T}{d_L+d_T}\right)^2$, and C_{ij} is the component of undamaged stiffness tensor.

After damage occurs, the material is still considered to be elastic and the damage response of the integration points is governed by the stiffness matrix reduction via updating damage variables given in Eq. (15).

2.4 Damage evolvement model

Damage initiation and damage evolution can be simulated by damage mechanism, which consists of failure criteria and damage evolution law. 2D braided composites comprise three phases: Fiber yarns, pure resin matrix and interface. Therefore, the failure mechanism contains three types: Yarn breaking, matrix cracking and interface debonding. In the present study, the damage mechanism of interface debonding is not considered.

Tsai-Wu criterion, implemented to predict the failure initiation and progression of braiding yarn, is given by

$$f(\sigma)-r_f=0 \tag{16}$$

where r_f is the damage threshold of braiding yarns. The expression of $f(\sigma)$ is given by

$$f(\sigma)=F_{11}\sigma_1^2+F_{22}\sigma_2^2+F_{33}\sigma_3^2+F_{44}\sigma_{23}^2+F_{55}\sigma_{13}^2+F_{66}\sigma_{12}^2+2F_{12}\sigma_1\sigma_2+2F_{13}\sigma_1\sigma_3+2F_{23}\sigma_2\sigma_3+F_1\sigma_1+F_2\sigma_2+F_3\sigma_3 \quad (17)$$

In Eq. (17)

$$F_{11}=\frac{1}{X_TX_C},\quad F_{22}=F_{33}=\frac{1}{X_TX_C}$$

$$F_{44}=\frac{1}{S_{23}^2},F_{55}=F_{66}=\frac{1}{S_{12}^2}$$

$$F_{12}=F_{13}=-\frac{1}{2}\sqrt{F_{11}F_{22}},F_{23}=-\frac{1}{2}\sqrt{F_{22}F_{33}}$$

$$F_1=\frac{1}{X_T}-\frac{1}{X_C},F_2=F_3=\frac{1}{Y_T}-\frac{1}{Y_C} \quad (18)$$

where X_T and X_C are the longitudinal tensile and compressive strengths of yarn; Y_T and Y_C are the transverse tensile and compressive strengths; S_{12} and S_{23} are the in-plane and out of plane strengths, respectively.

The Mises criterion is adopted as matrix failure criterion, namely

$$\frac{\sigma_{\mathrm{m}}^{\mathrm{ef}}}{\sigma_{\mathrm{m}}^{\mathrm{s}}}-r_{\mathrm{m}}=0 \quad (19)$$

where $\sigma_{\mathrm{m}}^{\mathrm{s}}$ is the tensile strength of matrix, r_{m} the damage threshold of matrix, and $\sigma_{\mathrm{m}}^{\mathrm{ef}}$ the effective stress of matrix and given by

$$\sigma_{\mathrm{m}}^{\mathrm{ef}}=(1/2((\sigma_1-\sigma_2)^2+(\sigma_1-\sigma_3)^2+(\sigma_3-\sigma_2)^2+3(\tau_{12}^2+\tau_{23}^2+\tau_{31}^2)))^{1/2} \quad (20)$$

The damage variables of yarns in Eq. (15) can be computed by[28]

$$D_i=1-\mathrm{e}^{\frac{1}{m}(1-r_f^m)} \qquad i=L,T,Z \quad (21)$$

where m is a softening parameter.

Damage variable of matrix has the similar form as Eq. (21), with $D_L=D_T=D_Z$.

The damage threshold r_i is initially set to 1.0 to represent initial elastic deformation and increases as damage accumulates analogous to plasticity model. It is defined as

$$r_i^j=f^{j-1} \qquad i=f,m \quad (22)$$

Damage accumulates and propagates when

$$\frac{\partial f}{\partial \varepsilon}\dot{\varepsilon}>0 \quad (23)$$

In Eqs. (22, 23), j is the index of strain increment step and $\dot{\varepsilon}$ the strain rate.

It is known that Tsai-Wu failure criterion is mode-independent. It identifies the failure progression, but cannot identify the failure modes of each yarn element. Thus, six indices, H_i ($i=1$—6), are defined to identify the failure modes of the failed elements, shown as

$$H_1=F_1\sigma_{11}+F_{11}\sigma_{11}^2,H_2=F_2\sigma_{22}+F_{22}\sigma_{22}^2$$
$$H_3=F_3\sigma_{33}+F_{33}\sigma_{33}^2,H_4=F_{44}\sigma_{23}^2 \quad (24)$$
$$H_5=F_{55}\sigma_{13}^2,H_6=F_{66}\sigma_{12}^2$$

At failure, the maximum one of the six indices H_i($i=1$—6) is assumed to identify the dominant failure mode. Failure index H_1 indicates yarn L breaking, H_2 and H_3 indicate transverse matrix cracking, and H_4, H_5 and H_6 indicate T-Z, L-Z and L-T shear failure modes of matrix.

2.5 Failure analysis process

The above constitutive theory and progressive damage simulation approach are implemented into a user defined material subroutine (UMAT), available in finite element software ABAQUS. During each strain increment, the stress level and damage station are calculated at the integration points of the elements. Once the failure criterion is satisfied, the stiffness reduction is carried out by updating the damage variables. The reduced stiffness is used for further analysis until the final increment step. Fig. 8 presents the flow chart of the failure analysis process.

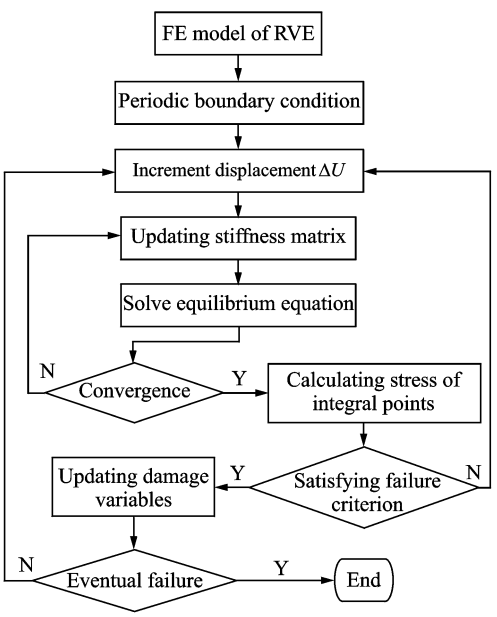

Fig. 8 Flow chart of failure analysis

3 RESULTS AND DISCUSSION

In order to verify the damage simulation method and reveal the damage mechanism of 2D braided composites, the tensile experimental results of specimen CE3 from Ref. [2] are selected for comparison study. Tensile tests of specimen CE3 are carried out on Instron Universal Testing Machine at a crosshead speed of 1 mm/min and at room temperature. The elastic properties of the component materials, including T300 carbon fiber and epoxy resin, are listed in Table 1. The tensile strength of T300 fiber is 2 480 MPa; the tensile and shear strength of epoxy resin are 64 MPa and 110 MPa. Table 2 gives the geometrical parameters of specimen CE3, used to establish the RVE model. The width of braiding yarn is divided into three parts and $a : b = 1 : 2$ is assumed in the present study.

Table 1 Elastic properties of fiber and matrix

Material	E_L/GPa	E_T/GPa	E_{LT}/GPa	G_{TT}/GPa	V_{LT}
T-300	230	40	24	14.3	0.26
Epoxy	3.5	3.5	1.3	1.3	0.35

Table 2 Geometrical parameters of specimen

Specimen	Geometrical parameter /mm				α	K'	V_f/%
	W	g	t_b	T			
CE3	1.04	0.15	0.34	0.92	17	0.79	44.6

According to the meshing requirement of FEM, element size needs to keep small at the edges of the intersecting yarns and resin matrix pocket. In this study, the FEM model consists of 8 438 nodes and 42 136 linear tetrahedron elements. Relatively fine meshing size is required to obtain more accurate stress distribution, especially near the boundaries of RVE. The mesh is checked for distortion and a mesh sensitivity analysis is performed. Note that the meshing size of the model in this study is fine enough and sufficient to guarantee the convergence of the solutions.

The small gaps between the adjacent yarns existing in the specimen are not considered in establishing the RVE model. Since the fiber-volume fraction of the composites will be too large when the actual fiber-volume fraction of yarn is adopted, thus the revised method proposed in Ref. [6] is used here, namely

$$\kappa = \frac{W}{W+g}\kappa' \tag{25}$$

The softening response relies heavily on the manufacture architecture and test conditions, which can lead to very scattered results. Consequently, the choice of softening parameters for each mode is still an open issue. As pointed out in Refs. [28-29], smaller values of m make the material behavior more ductile whereas higher values make the material behavior more brittle. In present study, $m_1 = 5$, $m_2 = 0.5$ and $m_3 = 0.5$ are selected as softening values for yarns damage of longitudinal fiber breaking, transverse matrix cracking, and shear failure, respectively.

3.1 Stress-strain curve

To obtain the macroscopic stress-strain curve of the material, the homogenization approach is employed in this study. The heterogeneous composites in the micro-scale are considered a homogeneous material in the macro-scale. The average stresses and strains in a RVE are defined by[24]

$$\bar{\sigma}_{ij} = \frac{1}{V}\int_V \sigma_{ij}\,\mathrm{d}V, \quad \bar{\varepsilon}_{ij} = \frac{1}{V}\int_V \varepsilon_{ij}\,\mathrm{d}V \tag{26}$$

where V is the volume of RVE.

Aggarwal et al[2] studied the mechanical properties of 2D braided composites with small braid angles of both cut- and uncut-edge configurations. Cut-edge specimens from a large composite panel lose fiber continuity at the edges, which affects the tensile behavior significantly. Because the edge effect is not considered in the present RVE, the applicability of the present damage model is restricted to the cut configuration. Thus, only the experimental result of cut specimen CE3 is picked up from Ref. [2].

A comparison of experimental and simulaton stress-strain curves is shown in Fig. 9. Note that the experimental data shows nonlinear constitutive character to some extent before sudden brittle failures, but the simulation results show al-

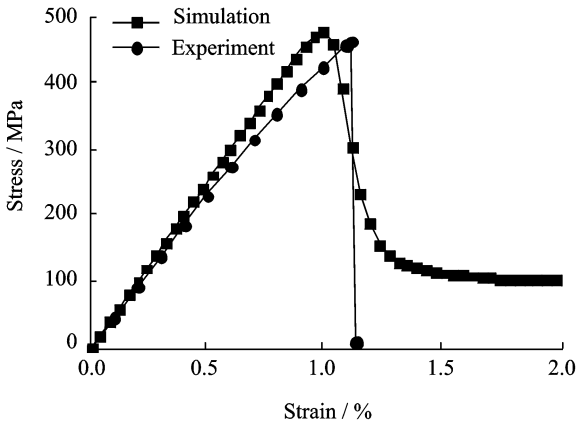

Fig. 9 Comparison of simulation and experimental results under uniaxial tension

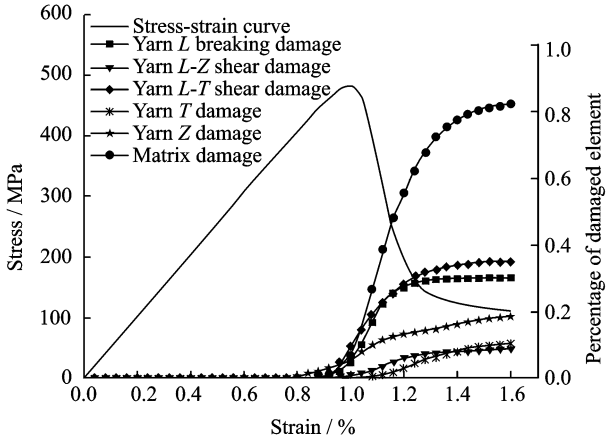

Fig. 10 Percentage of damage modes of yarn and matrix elements corresponding to tension process

most linear constitutive relationship until failure. This can be attributed to the initial manufacturing defects, such as micro-cracks in yarns and voids in matrix, but not considered in the RVE model. After reaching the maximum stress, the predicted curve decreases rapidly to a low plateau stress and the specimen loses the load carrying capacity. The predicted tensile strength and failure strain are 484 MPa and 1.0% and are consistent with the experimental strength 470 MPa and failure strain 1.12%, indicating that the damage modes applied to the yarns and matrix are reasonably accurate. The extended unloading observed in the computed stress-strain curves is most likely a numerical artifact, as the experimental specimens most likely have a more brittle fiber failure, while the computed curves have a more gradual unloading to promote numerical stability[19].

3.2 Damage propagation simulation

Fig. 10 shows the element damage percentage of braiding yarns and matrix corresponding to the stress-strain curve of the 2D braided composites. The element damage percentage is calculated via dividing the damaged element number by the constituents' element number of RVE. In the simulation process, the *T*-*Z* damage elements are very few, for simplify, this damage mode is not presented in Fig. 10.

With the increment of tensile loading, various failure modes occur, promote and couple with each other gradually. The whole progressive damage process can be divided into three periods. (1) Damage initiation period ($0.80\% \leqslant \varepsilon < 0.92\%$). At $\varepsilon = 0.80\%$, yarn *Z* damage mode is initially detected in the undulate zones of the yarns and damage initiates in the matrix pockets at $\varepsilon = 0.88\%$. Overall, in this period, the ratio of failure elements is fewer than 2%, which has less influence on the macro stress-strain curve. (2) Damage accumulation period ($0.92\% \leqslant \varepsilon < 1.02\%$). A variety of damage modes occur and accumulate continuously in this period, and the slope of the tensile stress-strain curve begins to decrease. At $\varepsilon = 1.00\%$, the stress-strain curve reaches the peak value, defined as the strength of the composites. At this time, the *L* breaking and *L*-*T* shear damage element percentages are 4.85% and 9.57%, respectively. (3) Damage propagation period $\varepsilon \geqslant 1.02\%$. All the damage modes spread rapidly; especially the *L* breaking and *L*-*T* shear damage modes of yarn and matrix damage, which lead to a sudden drop of the stress-strain curve. It is obvious that they are the main failure modes and control the mechanical response of the braided composites. Because of the failure of yarns, matrix pockets bear the greater amount of loads; therefore, the failure element percentage of matrix ascends faster than other damage modes. All of these analysis results agree well with the experimental findings in Ref. [2].

Since the main failure modes of the braided

composites are the L tensile breaking, planar L-T shear damage of yarn and matrix damage, it is of great significance to analyze the damage distribution and expansion trend. Fig. 11 depicts the expansion of L tensile breaking and L-T shear damage in one-directional braid yarns and matrix damage under different strain increments. It is found that these two kinds of damage occur initially in the undulate zones where two directional yarns cross with each other; and then damages develop rapidly along the braiding yarn direction. The damage value equalling to one in the L breaking elements indicates that this damage is serious. In contrast, just small parts of L-T shear damage elements are displayed with the damage value of one. Therefore, these materials have further load carrying capacity. It is exhibited that the matrix damages, developed in the matrix regions neighboring yarns intersecting zones, appear later than yarn damages.

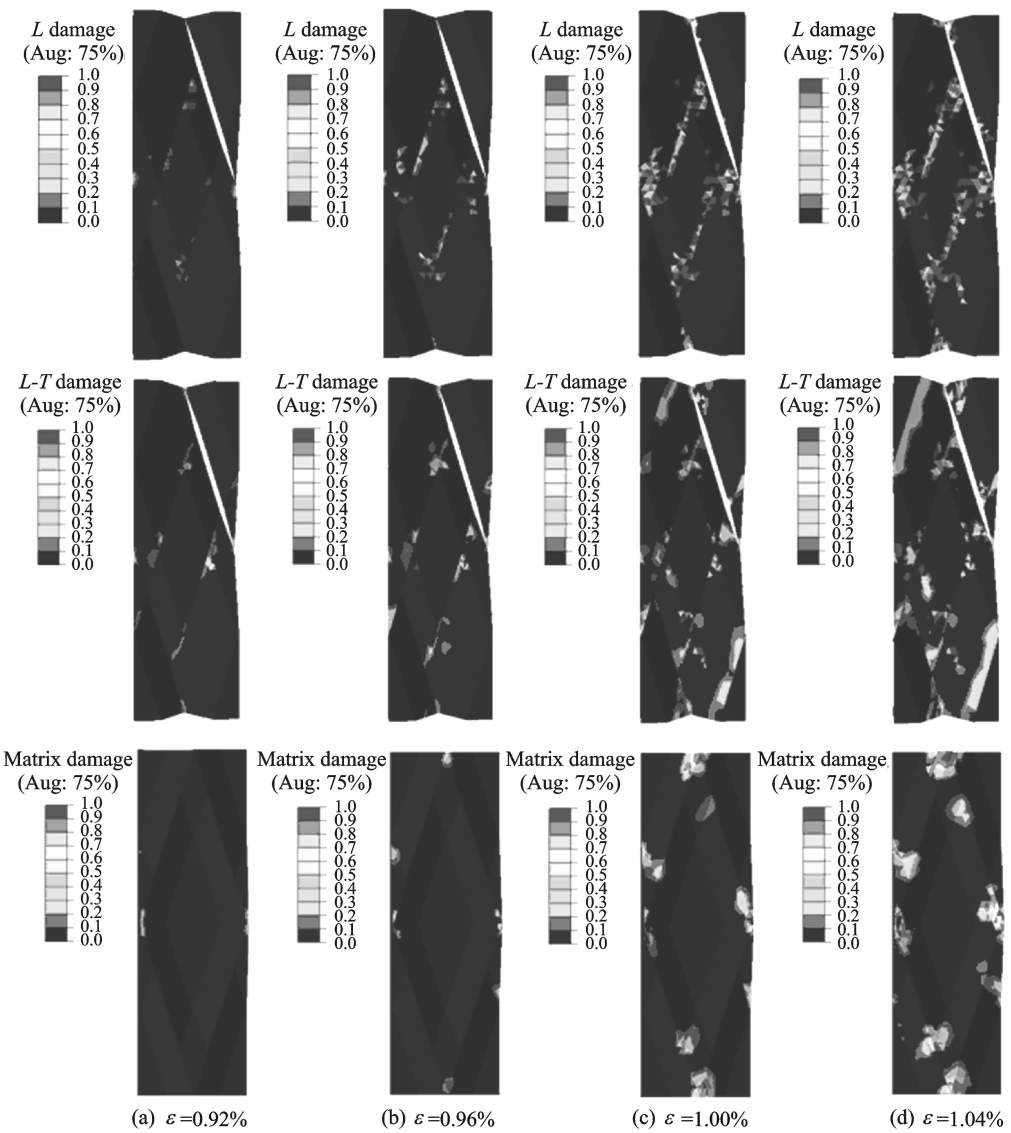

Fig. 11 Damage evolution

4 CONCLUSIONS

(1) The spatial configuration and the mutual squeezing of the yarns are validly reflected in RVE.

(2) The main failure modes of the 1×1 braided composites with small braid angle under tensile loading are the L tensile breaking, planar L-T shear modes of yarn and matrix damage.

(3) By adopting the average method, the macro stress-strain curve is simulated, from which the ultimate strength and failure strain are obtained. The numerical results show good agreement with available experimental data, thus validates the effectiveness of the damage simulation model.

References:

[1] Aggarwal A, Mmakrishna S, Ganesh V K. Predicting the in-plane elastic constants of diamond braided composites[J]. Journal of Composite Materials, 2001, 35(8): 665-687.

[2] Aggarwal A, Mmakrishna S, Ganesh V K. Predicting the strength of diamond braided composites[J]. Journal of Composite Materials, 2002, 36(5): 625-642.

[3] Byun J H. The analytical characterization of 2-D braided textile composites[J]. Composites Science and Technology, 2000, 60(5): 705-716.

[4] Masters J E, Foye R L, Pastore C M, et al. Mechanical properties of triaxially braided composites: Experimental and analytical results[J]. Journal of Composites Technology and Research, 1993, 15(2): 112-122.

[5] Quek S C, Waas A M, Shahwan K W, et al. Analysis of 2D triaxial flat braided textile composites[J]. International Journal of Mechanical Sciences, 2003, 45(6): 1077-1096.

[6] Zhang Chao, Xu Xiwu. Geometrical model and elastic properties prediction of 2D biaxial braided composites[J]. Acta Materiae Compositae Sinica, 2010, 27(5): 129-135. (in Chinese)

[7] Sun H Y, Qiao X. Prediction of mechanical properties of three dimensionally braided composites[J]. Composites Science and Technology, 1997, 57(6): 623-629.

[8] Shokrieh M M, Mazloomi M S. An analytical method for calculating stiffness of two dimensional tri axial braided composites[J]. Composite Structures, 2010, 92(12): 2901-2905.

[9] Carey J, Munro M, Fahim A. Longitudinal elastic modulus prediction of a 2-D braided fiber composite [J]. Journal of Reinforced Plastics and Composites, 2003, 22(9): 813-831.

[10] Goyal D, Tang X D, Whitcomb J D. Effect of various parameters on effective engineering properties of 2×2 braided composites[J]. Mechanics of Advanced Materials and Structures, 2005, 12(2): 113-128.

[11] Xu K, Xu X W. Finite element analysis of mechanical properties of 3D five-directional braided composites[J]. Materials Science and Engineering A, 2008, 487(1/2): 499-509.

[12] Tsai K H, Hwan C L, Chen W L, et al. A parallelogram spring model for predicting the effective elastic properties of 2D braided composites[J]. Composite Structures, 2008, 83(3): 273-283.

[13] Potluri P, Manan A. Mechanics of non-orthogonally interlaced textile composites[J]. Composites Part A, 2007, 38(4): 1216-1226.

[14] Tang X D, Whitcomb J D, Kelkar A D, et al. Progressive failure analysis of 2×2 braided composites exhibiting multiscale heterogeneity[J]. Composites Science and Technology, 2006, 66(14): 2580-2590.

[15] Quek S C, Waas A M, Shahwan K W, et al. Compressive response and failure of braided composites: Part 1—Experiments[J]. International Journal of Non-Linear Mechanics, 2004, 39(4): 635-648.

[16] Quek S C, Waas A M, Shahwan K W, et al. Compressive response and failure of braided composites: Part 2—Computations[J]. International Journal of Non-Linear Mechanics, 2004, 39(4): 649-663.

[17] Song S, Waas A W, Shahwan K W, et al. Braided textile composites under compressive loads: Modeling the response, strength and degradation[J]. Composites Science and Technology, 2007, 67(15): 3059-3070.

[18] Song S J, Waas A M, Shanwan K W, et al. Compression response of 2D braided textile composites: Single cell and multiple cell micromechanics based strength predictions[J]. Journal of Composite Materials, 2008, 42(23): 2461-2482.

[19] Li X T, Binienda W K, Goldberg R K. Finite element model for failure study of two dimensional triaxially braided composite[J]. Journal of Aerospace Engineering, 2010, 24(2): 170-180.

[20] Zeng T, Wu L Z, Guo L C. A finite element model for failure analysis of 3D braided composites[J]. Materials Science and Engineering A, 2004, 366(1): 144-151.

[21] Fang G D, Liang J, Wang B L. Progressive damage and nonlinear analysis of 3D four directional braided composites under unidirectional tension[J]. Composite Structures, 2009, 89(1): 126-133.

[22] Dong J W, Feng M L. Damage simulation for 3D braided composites byhomogenization method [J]. Chinese Journal of Aeronautics, 2010, 23(6): 677-685.

[23] Ayranci C, Carey J. 2D braided composites: A review for stiffness critical applications[J]. Composite Structures, 2008, 85(1): 43-58.

[24] Xia Z H, Zhou C W, Yong Q L, et al. On selection of repeated unit cell model and application of unified periodic boundary conditions in micro mechanical analysis of composites [J]. International Journal of Solids and Structures, 2006, 43(2): 266-278.

[25] Chamis C C. Mechanics of composites materials: Past, present and future[J]. Journal of Composites Technology and Research, 1989, 11(1): 3-14.

[26] Murakami S. Mechanical modeling of material damage[J]. Journal of Applied Mechanics, 1988, 55(2): 280-286.

[27] Zako M, Uetsuji Y, Kurashiki T. Finite element analysis of damaged woven fabric composite materials [J]. Composites Science and Technology, 2003, 63 (3/4): 507-516.

[28] Xiao J R, Gama B A, Gillespie J W. Progressive damage and delamination in plain weave S-2 Glass/SC-15 composites under quasi-static punch-shear loading [J]. Composite Structures, 2007, 78 (2): 182-196.

[29] Williams K V, Vaziri R. Application of a damage mechanics model for predicting the impact response of composite materials [J]. Computers and Structures, 2001, 79(10): 997-1011.